

Electronic Supplementary Information

Enhanced Li⁺ Conduction in Perovskite $\text{Li}_{3x}\text{La}_{2/3-x}\text{TiO}_3$ Solid-electrolyte via Microstructural Engineering

Woo Ju Kwon,^{a,b,†} Hyeongil Kim,^{c,†} Kyu-Nam Jung,^a Woosuk Cho,^c Sung Hyun Kim,^b Jong-Won Lee,^{a,d,} Min-Sik Park^{e,*}*

^a New and Renewable Energy Research Division, Korea Institute of Energy Research, 152 Gajeong-ro, Yuseong-gu, Daejeon 34129, Republic of Korea. E-mail: jjong277@kier.re.kr

^b Department of Chemical and Biological Engineering, Korea University, 145 Anam-ro, Seongbuk-gu, Seoul, 02841, Republic of Korea

^c Advanced Batteries Research Center, Korea Electronics Technology Institute, 25 Saenari-ro, Bundang-gu, Seongnam 13509, Republic of Korea.

^d Department of Advanced Energy and Technology, Korea University of Science and Technology (UST), 217 Gajeong-ro, Yuseong-gu, Daejeon 34113, Republic of Korea.

^e Department of Advanced Materials Engineering for Information and Electronics, Kyung Hee University, 1732 Deogyong-daero, Giheung-gu, Yongin 17104, Republic of Korea. E-mail: mspark@khu.ac.kr

† These authors contributed equally to this work.

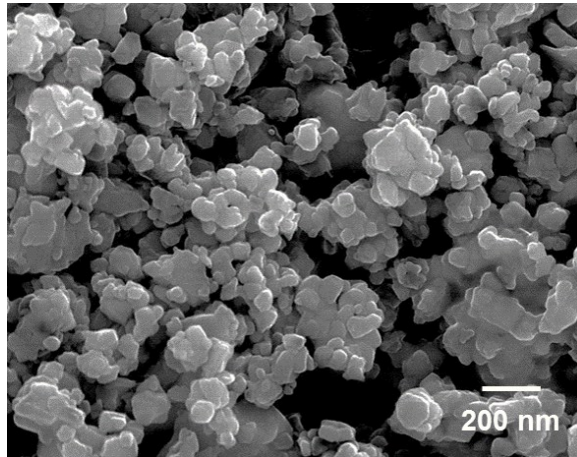


Fig. S1. A FESEM micrograph of the LLTO powder synthesized by the Pechini method and calcined at 900 °C.

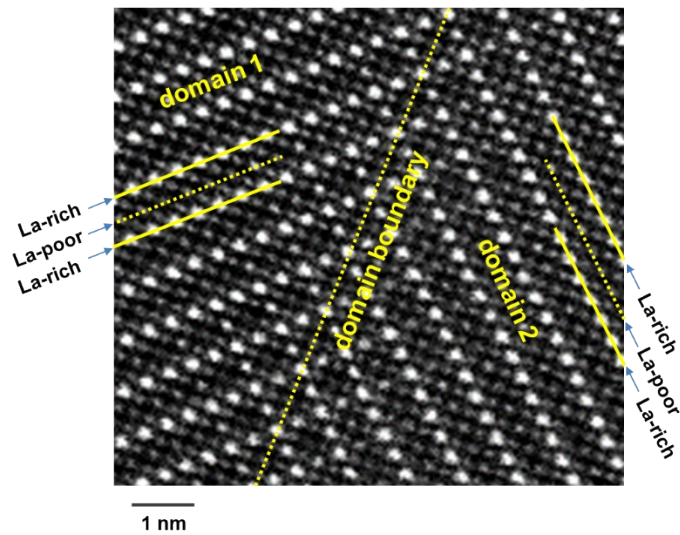


Fig. S2. HRTEM image of high-T LLTO; bright spots correspond to La-rich layers in “domain 1” and “domain 2”, and domains 1 and 2 meeting at the boundary are oriented $\sim 90^\circ$ to each other.

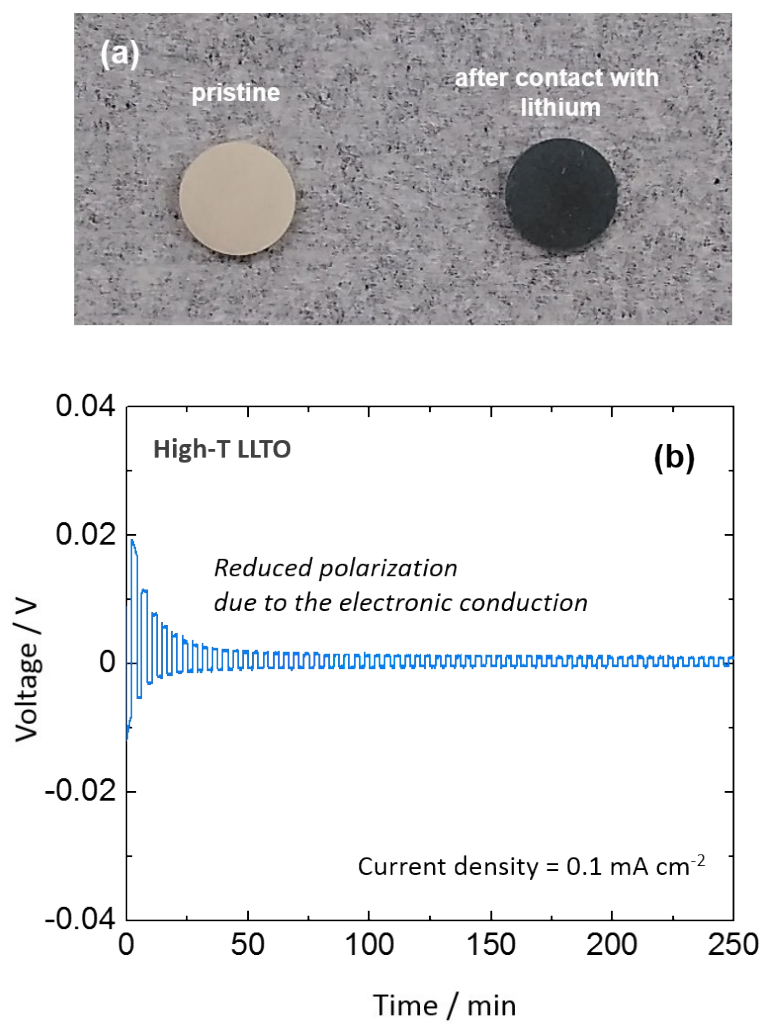


Fig. S3. (a) Photographs of the high-T LLTO electrolytes before and after contact with metallic lithium. (b) Cycling performance of the symmetric (Li | high-T LLTO | Li) cell measured at a current density of 0.1 mA cm⁻².

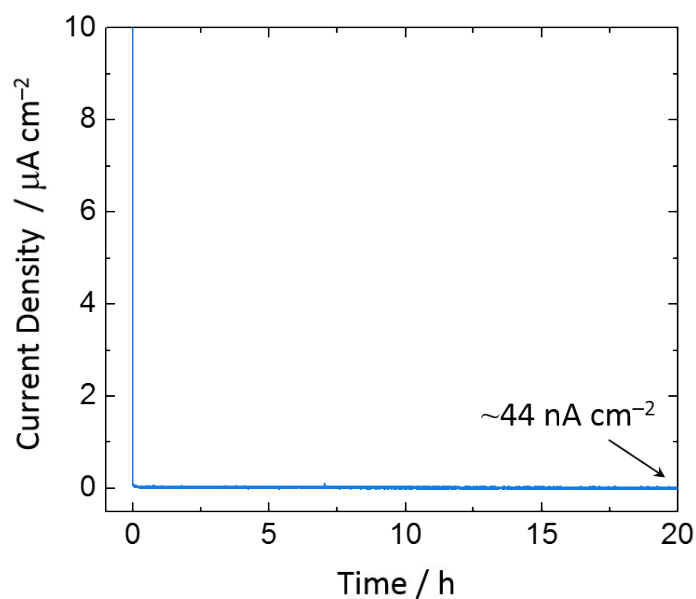


Fig. S4. Current vs. time profile of the high-T LLTO electrolyte measured by applying a constant voltage of 3.0 V. The measurement was performed at 25 °C.

The electronic conductivity was measured by a dc polarization method as reported elsewhere.³⁹ Both sides of the solid electrolyte were sputtered with Au (ion-blocking electrode), and then, the current vs. time profile was measured by applying a constant potential of 3.0 V. As shown in Fig. S4, the resulting current decreases rapidly with time and reaches a steady-state value ($\sim 4.4 \times 10^{-8} \text{ A cm}^{-2}$), which corresponds to the electronic current. From the steady-state current, the electronic conductivity was estimated to be $\sim 1.2 \times 10^{-9} \text{ S cm}^{-1}$. As a result, the Li^+ transference number was > 0.99999 , which confirms that the σ_{total} value is determined by Li^+ conduction.

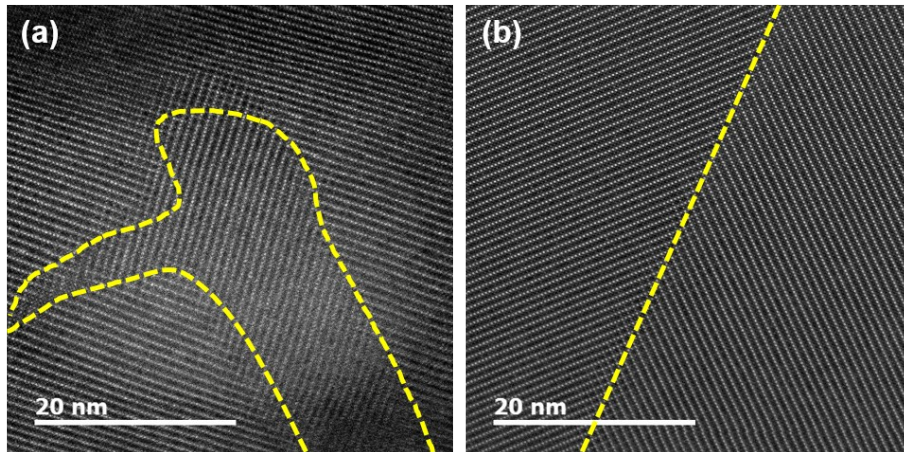


Fig. S5. TEM images of (a) low-T LLTO and (b) high-T LLTO; the dashed lines indicate domain boundaries in the microstructures of LLTO.

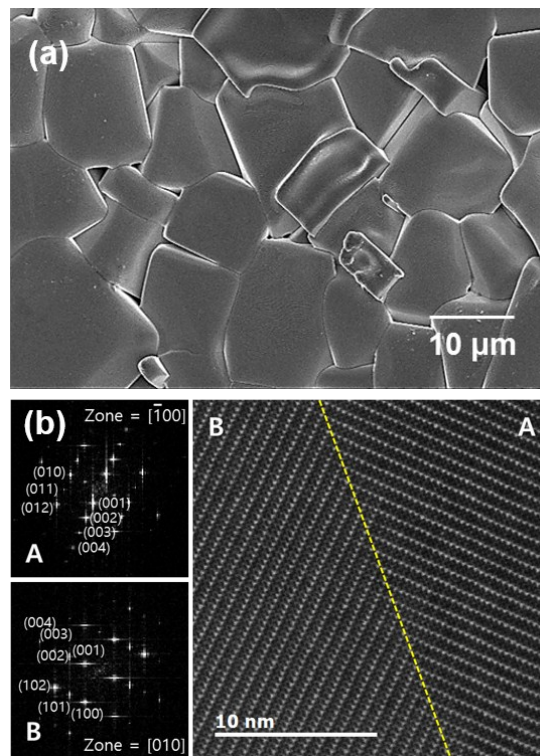


Fig. S6. (a) FESEM and (b) HRTEM micrograph combined with corresponding SADPs collected from different domains of Li-excess LLTO.

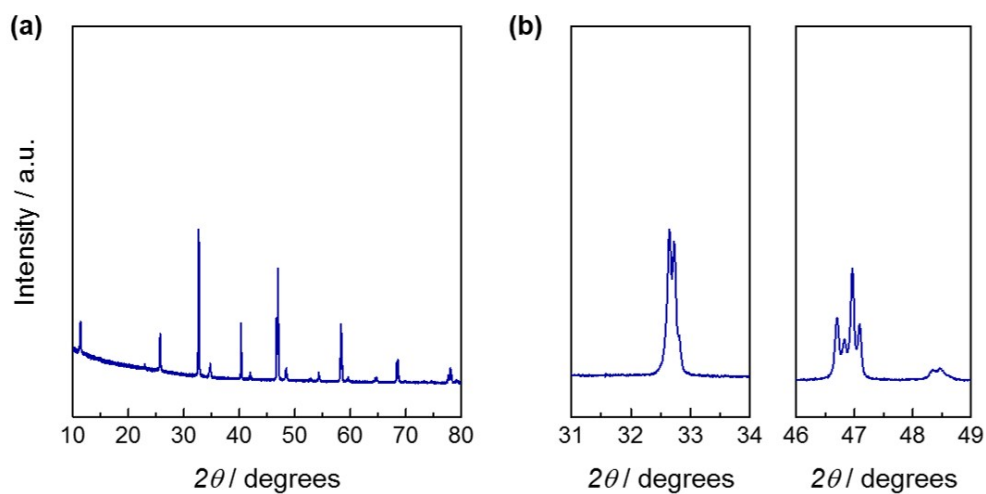


Fig. S7. (a) Powder XRD patterns of Li-excess LLTO. The magnified XRD patterns of Li-excess LLTO in 2 theta ranging from (b) 31° to 34° and 46° to 49°.

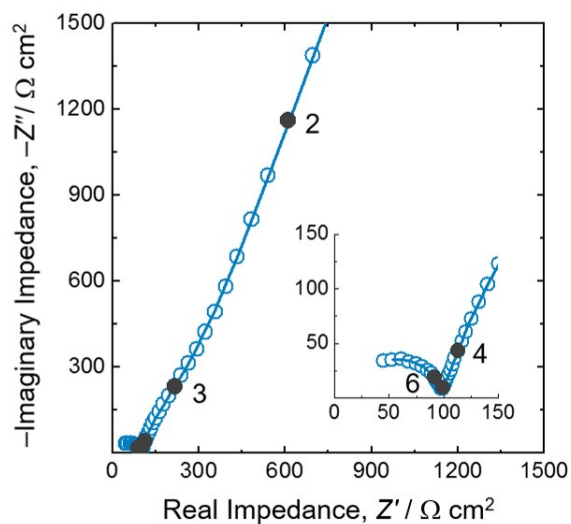


Fig. S8. Nyquist plot of the ac-impedance spectrum measured on Li-excess LLTO at 25 °C. The solid line represents the result fitted using the equivalent circuit in Figure 2a. Numbers on the closed circles indicate logarithmic frequency values.

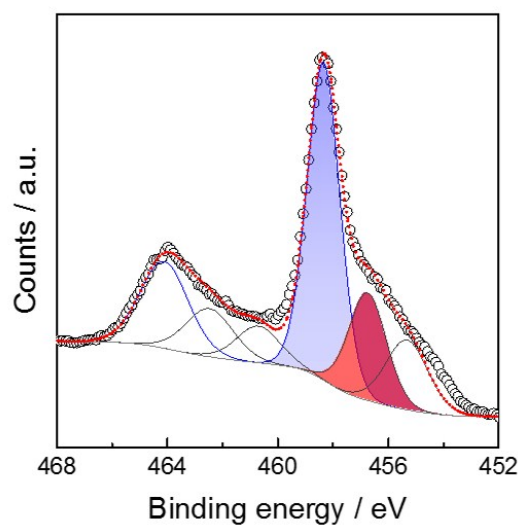


Fig. S9. XPS Ti 3d spectrum of Li-excess LLTO synthesized at a temperature of 1400°C.

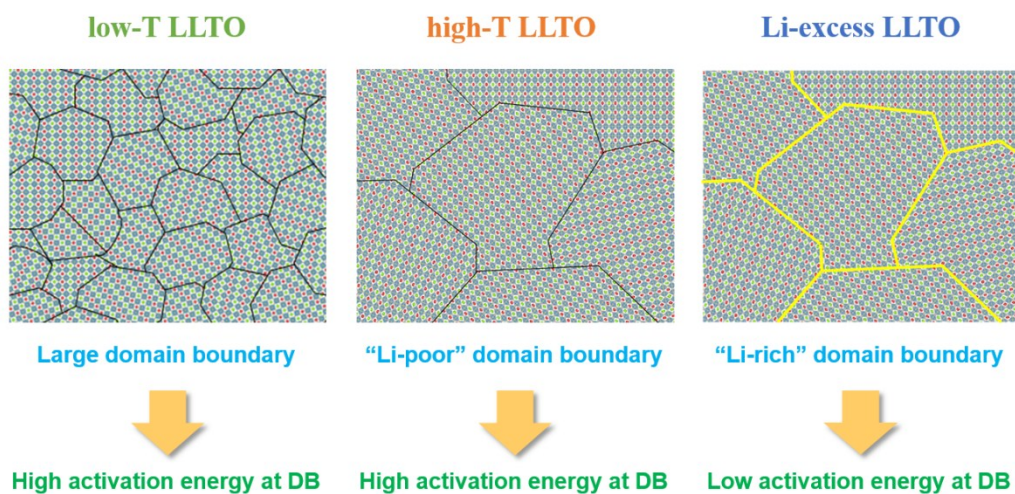


Fig. S10. Schematics of the domain microstructures of the LLTO electrolytes: low-T LLTO, high-T LLTO and Li-excess LLTO.